

NANOOPTICS

PACS numbers: 42.50.Wk; 87.80.Cc; 61.46.–w
DOI: 10.1070/QE2012v042n04ABEH014740

Optical forces in plasmonic nanoantennas

A.S. Shalin, S.V. Sukhov

Abstract. **The optical forces acting on nanoparticles in V-shaped plasmonic resonators with a high local-field gain have been investigated. Two versions are considered, which make it possible to implement either attractive or repulsive gradient optical forces. A plasmonic resonator is proposed, which can focus 350-nm radiation and implement a repulsive gradient force. It has been shown for the first time that a perturbation induced by a nanoparticle redistributes the field in the resonator so that additional intensity peaks arise in both versions to hold the nanoparticle in the resonator by forming an optical trap.**

Keywords: *nanoantenna, plasmonic resonator, optical force, optical trap, nanoparticle.*

1. Introduction

Currently, much attention has been given to the development of different methods for manipulating nano- and subnanoscale objects. Noteworthy is the constantly increasing number of studies devoted to the formation of optical traps [1, 2] and the analysis of optical forces arising in different systems [3, 4]. The reason is the high demand in nanosystems with specific physicochemical properties, which are applied in different fields of science and technology.

It was shown for the first time in [5] that a highly focused laser beam can be used to hold and displace microparticles; based on this finding, the so-called optical tweezers were developed [6, 7]. Currently, optical traps are used as a tool for displacing nanoparticles [8] and some biological objects [6, 9] and as high-precision force meters. The smaller the mass of the object displaced, the higher the field intensity that is required to hold it in the illuminated region; this relationship is due to the thermal motion, which is characterised by the energy $k_B T$ and tends to disturb the particle from equilibrium. Accordingly, the range of applicability of this method in biology and medicine is somewhat limited, because beams with intensities safe for living organisms can be used to transport only fairly large objects, for example, cells.

A.S. Shalin Kotel'nikov Institute of Radio Engineering and Electronics (Ul'yanovsk Branch), Russian Academy of Sciences, ul. Goncharova 48, 432011 Ul'yanovsk, Russia; Ul'yanovsk State University, ul. L. Tolstogo 42, 432700 Ul'yanovsk, Russia; e-mail: shalin_a@rambler.ru;
S.V. Sukhov CREOL, The College of Optics and Photonics, University of Central Florida, Central Florida Blvd. 4000, 32816 Orlando, Florida, USA

Received 13 October 2011
Kvantovaya Elektronika **42** (4) 355–360 (2012)
Translated by Yu.P. Sin'kov

The optical forces acting on nanoparticles in inhomogeneous fields were investigated in [10, 11]. Such fields arise as a result of interaction of electromagnetic waves with a metal surface [10] or on the external surface of a waveguide [11]. Here, resonant plasmon effects play an important role. They allow one to reach higher intensities and, as a consequence, larger optical forces using relatively weak (3–10 mW m^{-2}) excitation fields.

In this study we investigated the optical forces acting on a nanoparticle in systems with plasmonic focusing of light in a region with linear sizes much smaller than the light wavelength. Surface plasmon waves, which arise in a number of metals and are collective oscillations of free electrons under external visible laser radiation, have wavelengths on the order of several tens of nanometers [12, 13]. Transformation of an incident electromagnetic wave into a plasmon wave, its focusing, and subsequent reverse transformation into light allow for giant local field amplification. The structures implementing this phenomenon are known in the literature as nanoantennas or light concentrators [14]; the interest in them constantly increases. Nanoantennas composed of closely spaced cones, spheres, and parallelepipeds, as well as bow-tie nanoantennas (triangular prisms spaced by less than several tens of nanometers) have been investigated theoretically [15–21] and experimentally [22–27]. If the excitation conditions are satisfied in a system of resonant plasmon oscillations, the field strength in the gap between the nanoantenna elements may exceed the incident field strength by a factor of 10^2–10^3.

Obviously, since the possibility of subwave focusing is determined by the plasmonic properties of structure, the occurrence and intensity of this effect depend strongly on the radiation wavelength and the nanoantenna parameters. For example, local field amplifications by factors of ~200, ~160, and ~1000 were obtained, respectively, in [15] (at a wavelength of 830 nm for a system composed of two gold rods with a rectangular cross section), in [19] (at a wavelength of 700 nm for gold prisms), and in [25] (between two gold probes of atomic-force microscopes). The radiation concentrators in the form of V-shaped grooves on the surface of plasmon-resonant metals [27–30] can easily be implemented in practice. Sondergaard et al. [27] were able to amplify the incident field strength by a factor of 22–23 at a wavelength of 620–670 nm for a gold substrate and by a factor of 27–29 at a wavelength of 550–570 nm for a silver substrate. Gramotnev et al. [28–30] proposed an analytical theory of similar plasmonic resonators and 'inverted' systems (Λ-shaped metal wedges), based on the geometric-optics approximation. However, this approach can be applied in a rather narrow range of opening angles (7°); at larger angles the results of the analytical theory and numerical analysis differ significantly. It was shown in

[28–30] that, at a wavelength of 632 nm, the local field in gold V-shaped grooves can be amplified by a factor of 38–40 at an opening angle of 14° and a groove depth of ~9.7 μm.

Thus, since the field intensity in such structures may exceed the incident-wave intensity by several orders of magnitude, the optical forces acting on the nanoparticle increase correspondingly. Note that the behaviour of nanoparticles placed inside a plasmonic resonator as well as the influence of the perturbation induced by them on the field distribution have not been investigated. This study may help to develop new methods for optical control of nanoobjects.

2. Basic equations

The expression for the electromagnetic force F acting on a rigid body in the field of external radiation can be obtained based on the conservation law for the total momentum of the system [31, 32]:

$$\langle \boldsymbol{F} \rangle = \int_{\Sigma} \langle \hat{T}(\boldsymbol{r},t) \rangle \boldsymbol{n}(\boldsymbol{r}) \mathrm{d}\sigma, \quad (1)$$

where $\boldsymbol{n}$ is the external normal to the surface Σ; $\langle \hat{T}(\boldsymbol{r},t) \rangle$ is the energy–momentum tensor in vacuum (Maxwell stress tensor),

$$\langle T_{\alpha\beta} \rangle = \frac{1}{2} \mathrm{Re} \left[\varepsilon_0 E_\alpha E_\beta^* + \frac{1}{\mu_0} B_\alpha B_\beta^* - \frac{1}{2} \left(\varepsilon_0 |\boldsymbol{E}|^2 + \frac{1}{\mu_0} |\boldsymbol{B}|^2 \right) \delta_{\alpha\beta} \right]; \quad (2)$$

$\alpha, \beta = x, y, z$; $\boldsymbol{E}$ and $\boldsymbol{B}$ are, respectively, the vectors of electric field strength and magnetic induction, determined on an arbitrary surface Σ covering the body; and ε_0 and μ_0 are, respectively, the permittivity and permeability of vacuum.

Note that the electric and magnetic fields entering (2) are total and take into account the fields scattered by the objects under study; in this case, ratio (1) for a body in vacuum can easily be transformed into the ratios for a body placed in some medium by means of the following replacements: $\varepsilon_0 \to \varepsilon\varepsilon_0$ and $\mu_0 \to \mu\mu_0$ (with the dispersion of the medium neglected) [31].

If the body under consideration is small in comparison with the wavelength, expression (2) can be significantly simplified [32], and the electromagnetic force takes the form

$$\boldsymbol{F} = \frac{\alpha_\mathrm{p}'}{4} \nabla |\boldsymbol{E}_\mathrm{eff}|^2 + \frac{\alpha_\mathrm{p}''}{2} |\boldsymbol{E}_\mathrm{eff}|^2 \nabla\varphi, \quad (3)$$

where $\alpha_\mathrm{p} = \alpha_\mathrm{p}' + \mathrm{i}\alpha_\mathrm{p}''$ is the polarisability of a nanoparticle, $\boldsymbol{E}_\mathrm{eff}(\boldsymbol{r},t) = \boldsymbol{e}|\boldsymbol{E}_\mathrm{eff}|\exp(\mathrm{i}\varphi - \mathrm{i}\omega t)$ is the total field incident on it, and $\boldsymbol{e}$ is the polarisation vector for $\boldsymbol{E}_\mathrm{eff}$. Note that, in contrast to the field $\boldsymbol{E}$, which enters expression (2), $\boldsymbol{E}_\mathrm{eff}$ does not take into account the field emitted by the particle. Thus, the total force exerted by the electromagnetic wave on the nanoparticle is separated into two components: the gradient force [the first term in the right-hand side of (3)], which depends on the real part of the nanoparticle polarisability and acts in the direction of increasing field intensity, and the scattering force [the second term on the right-hand side of (3)], which depends on the imaginary part of the polarisability, acts in the direction of change in the field phase, and determines the radiation pressure. The scattering force is due to the wave-to-particle momentum transfer. If the particle is affected by only a plane wave, the direction of this force coincides with the electromagnetic wave propagation direction. According to formula (3), at $\alpha_\mathrm{p}' > 0$ the gradient force is directed toward the region of highest field intensity (from here on, we will refer to it as the attractive gradient force); in the opposite case, it is directed oppositely (repulsive gradient force).

The estimate of the work A of optical forces [which can easily be obtained from (3)],

$$A = \frac{\alpha_\mathrm{p}'}{4} \left(|\boldsymbol{E}_\mathrm{eff}^{(2)}|^2 - |\boldsymbol{E}_\mathrm{eff}^{(1)}|^2 \right) + \frac{\alpha_\mathrm{p}''}{2} \int \left(|\boldsymbol{E}_\mathrm{eff}(\boldsymbol{r})|^2 \nabla\varphi(\boldsymbol{r}) \right) \mathrm{d}\boldsymbol{r}, \quad (4)$$

shows that, in order to overcome thermal motion ($k_\mathrm{B}T \approx 4 \times 10^{-21}$ J at $T = 300$ K) and hold a particle several nanometres in size within the illuminated region, one needs a field intensity of 50–100 mW m^{-2} (depending on the particle parameters). In this context, the incident field is generally strongly focused to increase the electrodynamic forces; for example, the focused beam diameter in the aforementioned optical traps and tweezers does not exceed several tens of micrometers.

3. System with a repulsive gradient force

Let us determine the polarisability of a nanoparticle in the generally known form [12]:

$$\alpha_\mathrm{p} = 4\pi\varepsilon_0 a^3 \frac{\tilde{n}^2 - \tilde{n}_\mathrm{m}^2}{\tilde{n}^2 + 2\tilde{n}_\mathrm{m}^2} \quad (5)$$

where a is the radius of the particle, $\tilde{n}$ is its refractive index, and $\tilde{n}_\mathrm{m}$ is the refractive index of the ambient medium (vacuum in our case). Thus, the necessary condition for implementing the inequality $\mathrm{Re}\alpha_\mathrm{p} < 0$ and, therefore, a repulsive gradient force for a dielectric particle is the inequality $n < n_\mathrm{m}$. The experimentally investigated effect of capture of water microdrops in glycerol and paraffin [33] and hollow glass microspheres in water [34] by a shaped laser beam is based on this condition. Here, structured radiation is necessary to form closed regions with a low field intensity, into which a particle with negative polarisability can be captured. In vacuum or air ($n_\mathrm{m} = 1$), the real part of polarisability is negative, for example, for silver nanoparticles in the short-wavelength range of the plasmon peak. Note that currently silver appears to be the only material having this property in vacuum; other metals yield $\mathrm{Re}\alpha_\mathrm{p} < 0$ only in liquids.

Using the experimental data of [35] (with the corresponding size corrections [36]) for $\tilde{\varepsilon}$, we find the real part of polarisability of a silver nanocluster with a radius of 7–25 nm to have the largest (in modulus) negative value at a wavelength of ~350 nm.

Note that the data in the literature on the fabrication of nanoantennas with a vacuum resonant gap for radiation in the blue and UV spectral ranges are very scarce [18, 37]. Sondergaard et al. [27] derived an expression for the dependence of the resonant wavelength of a V-shaped groove on its depth, according to which the system under consideration should have a series of resonances (for different groove depths) at a wavelength of 350 nm. It was stated again in [38] that local field can be significantly amplified in the blue and UV ranges, although no specific calculations were presented.

We thoroughly investigated this problem by the finite-element method (using the Comsol Multiphysics 3.5a package); however, we failed to obtain any significant amplification (by a factor of more than 3–5) at this wavelength in a V-shaped resonator formed on metal surface. In this context, we propose a modified radiation concentrator (Fig. 1), which provides large gains for a local electromagnetic field in the blue spectral region. The resonator is a V-shaped groove on a dielectric surface, coated by a thin silver layer from inside.

Note that systems inverted with respect to the one under consideration were investigated previously (for example, in [39]) as applied to the theory of conical waveguides with a nanohole and metallised external surface. In this case, the field intensity in the region of narrowing the fiber was determined by its material; the largest values in the blue range were obtained for GaN. In the case under consideration the medium inside the nanoantenna is vacuum. Previously a significant amplification in the red and IR spectral ranges was obtained for a similar system with gold coating [40].

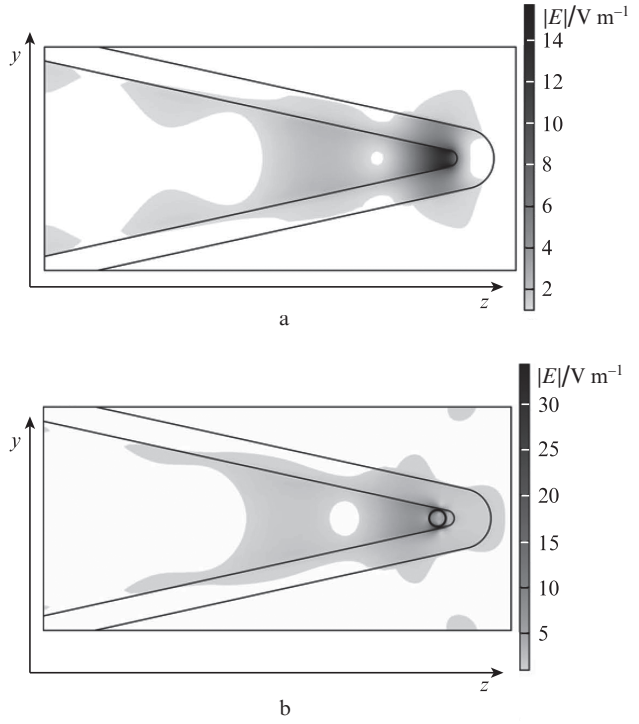

Figure 1. Distribution of the electric field modulus $|E|$ in a plasmonic resonator (a) without a particle and (b) in the presence of a silver nanoparticle with a radius $a = 5$ nm. The resonator is a V-shaped groove on the surface of a dielectric substrate with a refractive index $n_d = 2.3$, coated with a silver layer 16 nm thick. The groove depth $h = 1200$ nm; the opening angle $\beta = 25°$; and the inner and outer rounding radii of the bottom are 5 and 19 nm, respectively; there is vacuum inside the groove. An external field with a strength $E = 1$ V m^{-1} is incident in the direction of the z axis and is polarised along the y axis. The wavelength $\lambda = 350$ nm and the silver refractive index $n_{Ag} = 0.12 + i1.31$ [35].

Figure 1a shows the spatial distribution of the electric field modulus in the nanoantenna under study, which was obtained by exact numerical calculation [41]. According to the analysis performed, the maximum gain (about 14–18) is observed at several possible configurations of the system, which differ in the groove depth, opening angle, metal-film thicknesses, etc. In this study we will use the parameters listed in the caption to Fig. 1. Note also that the position of the field maximum along the z axis is determined by the structural parameters; therefore, this characteristic can also be optimised.

Figure 1b presents the field distribution in the presence of a silver nanoparticle. Obviously, the latter changes significantly the field distribution in the resonator. Since the field is highly inhomogeneous, one must use exact numerical calculation of the components of the Maxwell tension tensor (2).

For simplification, we will consider a two-dimensional geometry from here on and, therefore, calculate the linear densities of the values studied.

Figure 2 presents the results of calculating the total optical forces on silver nanoparticles with radii of 5, 10, and 15 nm. Although their polarisabilities are negative, the total optical force near the resonator bottom is positive (is directed along the z axis) and does not push the object out but, on the contrary, tends to hold it in near the bottom. The work that is done during the particle motion from the groove bottom to the surface is positive: $A_{Ag(5)} = 0.5 \times 10^{-6}$ rel. units m, $A_{Ag(10)} = 1.1 \times 10^{-6}$ rel. units m, and $A_{Ag(15)} = 1.3 \times 10^{-6}$ rel. units m. From here on, the work of the forces directed toward the resonator bottom (i.e., along the z axis) and, therefore, impeding the nanoparticle displacement to the input hole, is considered to be positive. Such an unusual behaviour of the optical forces is due to the interference of scattered and reflected fields, which gives rise to a stronger field peak before the particle (Fig. 3) and, therefore, a repulsive gradient force directed toward the groove bottom. In other words, the gradient optical force, as it was supposed, is directed toward the intensity minimum, and the occurrence of an additional peak before the particle impedes its motion, thus forming a stable trap near the bottom.

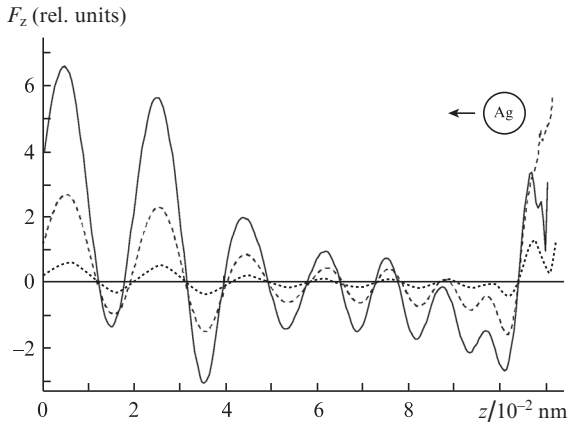

Figure 2. Total optical force (z-component) acting on silver nanoparticles with radii of (solid line) 15, (dashed line) 10, and (dotted line) 5 nm for the motion inside the plasmonic resonator presented in Fig. 1. The sign of the force determines its direction: the positive force is codirectional with the z axis, and the negative force is directed oppositely. The arrow indicates the motion direction (from the bottom of the groove to its surface). The positive force is directed toward the bottom and thus holds the nanoparticle in the resonator, while the negative force pushes the object to the surface. The parameters of the resonator and external field are the same as in Fig. 1.

With an increase in the distance from the bottom, the type of interference changes from constructive to destructive and vice versa, which leads to a change in the ratio of the field intensities before and behind the particle and, therefore, to a periodic change in the direction of the total acting force (Fig. 2). As the calculation shows, a particle contacting the walls of the resonator (independent of its distance from its bottom) is held near the bottom by the positive total electromagnetic force.

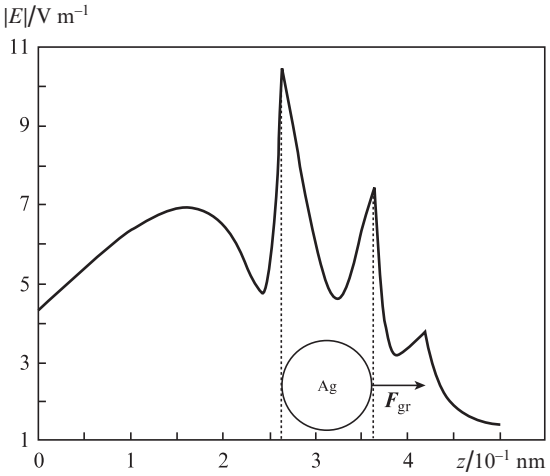

Figure 3. Distribution of the electric field modulus $|E|$ along the straight line oriented parallel to the z axis and passing through the center of a silver nanoparticle with a radius $a = 5$ nm, which corresponds to the initial position of the particle (see Fig. 1b). The arrow shows the direction in which the gradient optical force F_{gr} acts. The parameters of the resonator and external field are the same as in Fig. 1.

Thus, when the repulsive gradient force is used, the V-shaped resonator under study serves as an optical trap.

4. System with an attractive gradient force

According to formulas (3) and (5), an attractive gradient force (which occurs at $\mathrm{Re}\alpha_p > 0$) in the visible range is implemented for any dielectric, as well as for almost all conductors (except for the case considered in Section 3). In this context, since there is no limitation on the incident radiation wavelength, we will investigate the behaviour of nanoparticles and optical forces in the resonators whose parameters were reported in [27].

Figure 4 shows the field distribution in the aforementioned system at a wavelength of 632 nm; the resonator parameters are indicated in the caption.

We will now choose gold as a material for nanoparticles, because gold particles at this wavelength have a larger real part of polarisability in comparison with silver ones [for a cluster of radius $a = 10$ nm, $\alpha_{p(Au)} = 1.45 \times 10^{-34} + i4.4 \times 10^{-36}$ C m^2 V^{-1} and $\alpha_{p(Ag)} = 1.32 \times 10^{-34} + i6.3 \times 10^{-37}$ C m^2 V^{-1}], and, for comparison, dielectric TiO_2 nanoparticles [$n = 3$, $\alpha_{p(TiO_2)} = 8.09 \times 10^{-35}$ C m^2 V^{-1}].

The results of calculating the total optical force for gold and titanium dioxide particles with radii of 5, 10, and 15 nm are shown in Figs 5a and 5b, respectively. As for the system with a repulsive gradient force, the field is significantly redistributed, and a higher intensity peak is now observed from the side of the bottom (Fig. 6). Thus, the attractive gradient force tends to hold nanoparticles in the resonator. This statement is illustrated by Fig. 6, where the distribution of the electric field modulus is presented by analogy with Fig. 3. As previously, one can observe a periodic change in the sign of the total optical force and a change in the ratio of field intensities before and behind the particle, which is due to the character of field interference. The work done by this force during nanoparticle displacement from the bottom of the resonator to its surface takes the following values: $A_{Au(5)} = 1 \times 10^{-6}$ rel. units m, $A_{Au(10)} = 3 \times 10^{-6}$ rel. units m, $A_{Au(15)} = 2.8 \times 10^{-6}$ rel. units m,

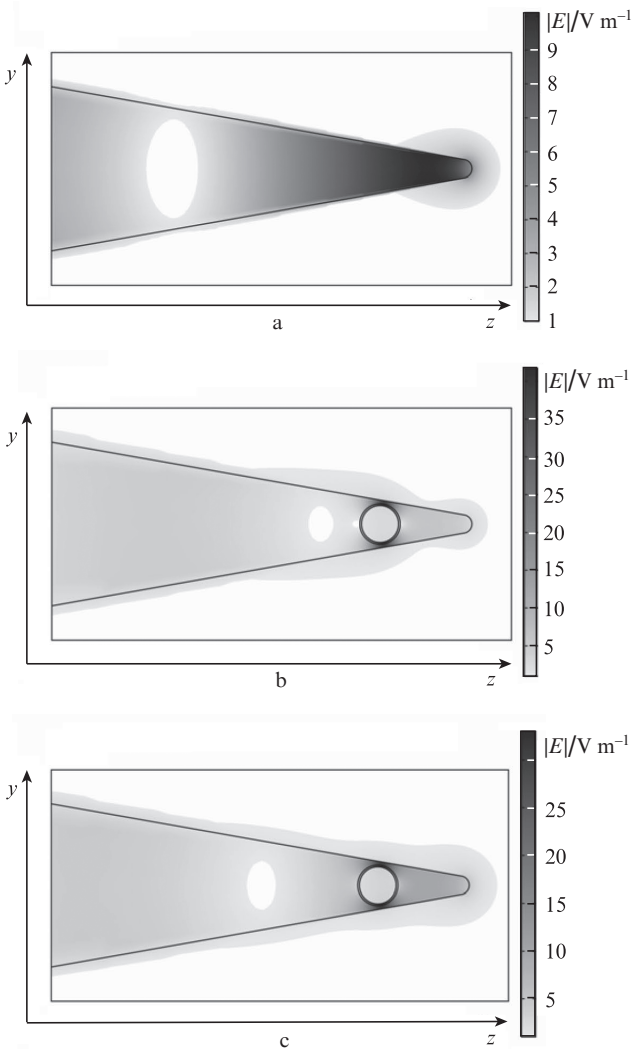

Figure 4. Distributions of the electric field modulus $|E|$ in a plasmonic resonator (a) without a particle, (b) containing a gold nanoparticle with a radius $a = 10$ nm, and (c) containing a TiO_2 nanoparticle with $a = 10$ nm. The resonator is a V-shaped groove on the surface of a bulk gold substrate. The groove depth $h = 700$ nm; the opening angle $\beta = 20°$; and the rounding radius of the bottom is 5 nm; there is vacuum inside the groove. An external field with a strength $E = 1$ V m^{-1} is directed along the z axis and polarised along the y axis. The wavelength is $\lambda = 632$ nm and the refractive indices are $n_{Au} = 0.18 + i3.42$ and $n_{TiO_2} = 3$ [35, 42].

$A_{TiO_2(5)} = 0.5 \times 10^{-6}$ rel. units m, $A_{TiO_2(10)} = 1.7 \times 10^{-6}$ rel. units m, and $A_{TiO_2(15)} = 1.7 \times 10^{-6}$ rel. units m.

Obviously, in each case considered above, a particle must overcome the potential barrier to leave the resonator; for the systems with a repulsive gradient force this barrier is somewhat lower. Thus, the above-considered system with plasmonic focusing of radiation is a stable trap for particles with both positive and negative real parts of polarisability.

5. Conclusions

We investigated the optical forces acting on nanoparticles in systems with subwave focusing of radiation, which yields high field intensities in regions with linear sizes much smaller than the light wavelength. Two structural versions were investigated (based on repulsive and attractive gradient forces). The parameters of the system at which 350-nm radiation is focused

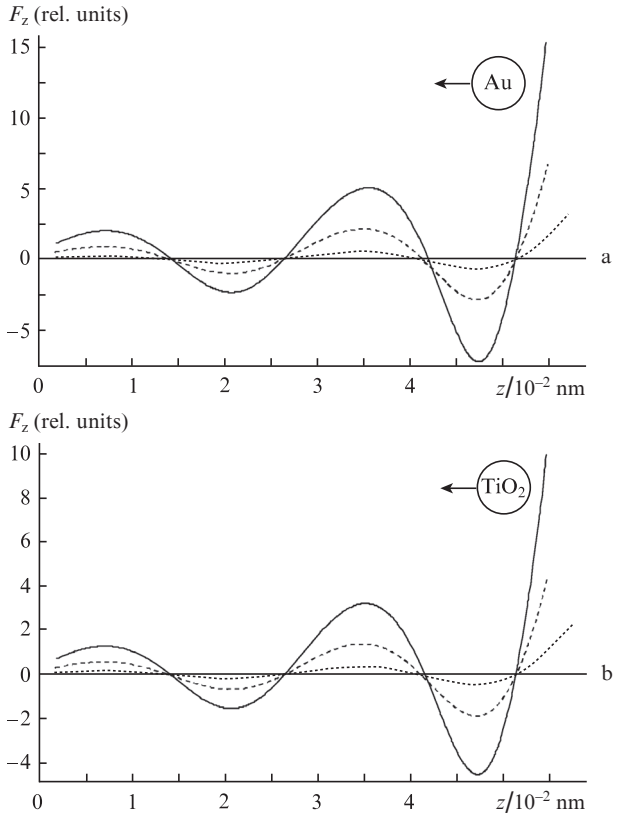

Figure 5. Total optical force (z-component) acting on (a) gold and (b) TiO_2 nanoparticles with radii of (solid line) 15, (dashed line) 10, and (dotted line) 5 nm for the motion inside the plasmonic resonator presented in Fig. 4. The sign of the force determines its direction: the positive force is codirectional with the z axis, while the negative force is directed oppositely. The arrow shows the direction motion (from the bottom of the groove to its surface). The parameters of the resonator and external field are the same as in Fig. 4.

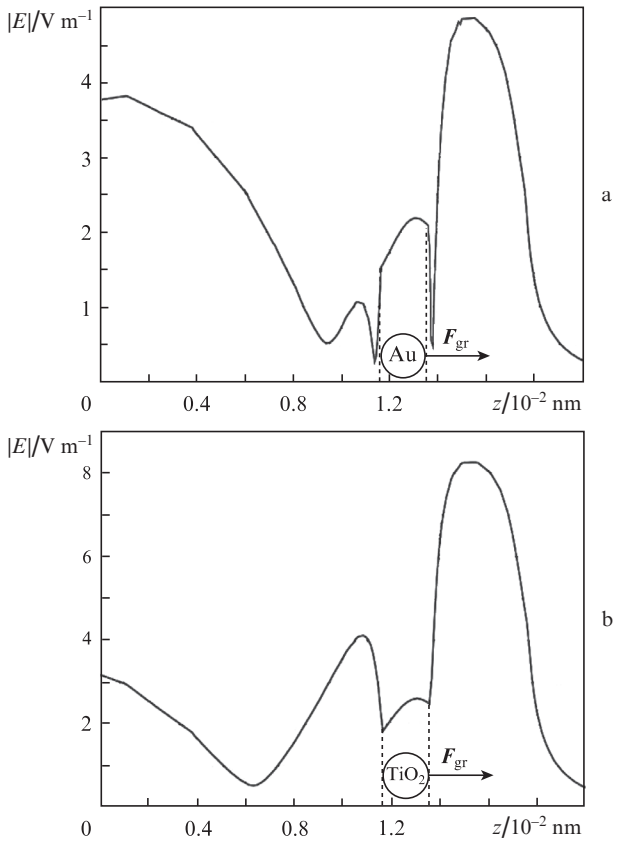

Figure 6. Distributions of the electric field modulus $|E|$ along the straight lines oriented parallel to the z axis and passing through the centers of (a) gold and (b) TiO_2 nanoparticles with radii $a = 10$ nm, which correspond to the initial positions of the particles (see Figs 4b, 4c). The arrow indicates the direction in which the gradient optical force F_{gr} acts. The parameters of the resonator and external field are the same as in Fig. 4.

were determined. In this case, the gradient optical force acting on a silver nanoparticle is directed toward the minimum field intensity. It is shown that the perturbation introduced by the particle into the field distribution in the resonator is fairly large and gives rise to additional intensity peaks, which impede nanoparticle displacement. In the case of a repulsive gradient force, an intensity peak arises before the particle to lock it near the resonator bottom; this peak is stronger than that behind the particle. In the case of an attractive gradient force the situation is reverse: a stronger peak arises near the bottom behind the particle to attract it. This effect is due to the contribution of the intrinsic field scattered by the particle and reflected from the resonator walls to the total field acting on the particle. As a result, an increase in the distance from the particle to the resonator bottom and walls leads to a change in the sign of the total optical force, in correspondence with the change in the character of interference from constructive to destructive and vice versa.

Thus, in the cases considered above, particles are captured (independent of their polarisability) into an optical trap near the resonator bottom. This effect can help to manipulate particles in microhydrodynamic capillaries. Particles moving along a V-shaped microchannel can effectively be driven to the bottom and stopped using weak external fields.

To implement the reverse effect (expulsion of an object from the groove), it is obviously necessary to change the character of field interference and, correspondingly, the sign of the acting force in the initial position of the particle. This can be done, for example, by making the nanoparticle levitate at some distance from the bottom due to the electrostatic forces; this situation was realised in [10].

References

1. Grier D.G. *Nature*, **424**, 810 (2003).
2. Wang K., Schonbrun E., Steinvurzel P., Crozier K.B. *Nature Commun.*, **2**, 469 (2011).
3. Huang L., Martin O.J.F. *Opt. Lett.*, **33**, 3001 (2008).
4. Juan M.L., Righini M., Quidant R. *Nature Photonics*, **5**, 349 (2011).
5. Ashkin A. *Proc. Natl. Acad. Sci. USA*, **94**, 4853 (1997).
6. Svoboda K., Block S.T. *Ann. Rev. Biophys. Biomol. Struct.*, **23**, 247 (1994).
7. Novotny L., Bian R.X., Xie X.S. *Phys. Rev. Lett.*, **79**, 645 (1997).
8. Righini M., Volpe G., Girard C., et al. *Phys. Rev. Lett.*, **100**, 186804 (2008).
9. Michael P. *Laser Tweezers in Cell Biology* (California: Acad. Press, 1998) Vol. 55.
10. Wang K., Schonbrun E., Crozier K.B. *Nano Lett.*, **9**, 2623 (2009).
11. Kawata S., Tani T. *Opt. Lett.*, **21**, 1768 (1996).

12. Mishchenko M.I., Travis L.D., Lacis A.A. *Scattering, Absorption and Emission of Light by Small Particles* (Cambridge: Cambridge Univ. Press, 2002).
13. Noginov M.A., Zhu G., Belgrave A.M., et al. *Nature*, **460**, 1110 (2009).
14. Schuller J.A., Barnard E.S., Cai W. *Nature Mater*., **9**, 193 (2010).
15. Muhlschlegel P., Eisler H.-J., Martin O.J.F., et al. *Science*, **308**, 1607 (2005).
16. Hyun-Joo Chang, Se-Heon Kim, Yong-Hee Lee, et al. *Opt. Express*, **18**, 24163 (2010).
17. Fei Zhou, Ye Liu, Zhi-Yuan Li, et al. *Opt. Express*, **18**, 13337 (2010).
18. Ding W., Bachelot R., Espiau de Lamaestre R., et al. *Opt. Express*, **17**, 21228 (2009).
19. Marty R., Baffou G., Arbouet A., et al. *Opt. Express*, **18**, 3035 (2010).
20. McMahon J.M., Gray S.K., Schatz G.C. *Nano Lett*., **10**, 3473 (2010).
21. Nome R.A., Guffey M.J., Scherer N.F., et al. *J. Phys. Chem. A*, **113**, 4408 (2009).
22. Yanik A.A., Adato R., Erramilli S., et al. *Opt. Express,* **17**, 20900 (2009).
23. Huang F., Baumberg J.J. *Nano Lett*., **10**, 1787 (2010).
24. Zhang W., Huang L., Santschi C., et al. *Nano Lett.*, **10**, 1006 (2010).
25. Ward D.R., Huser F., Pauly F., et al. *Nature Nanotech*., **5**, 732 (2010).
26. Bora M., Fasenfest B.J., Behymer E.M., et al. *Nano Lett.*, **10**, 2832 (2010).
27. Sondergaard T., Bozhevolnyi S.I., Beermann J., et al. *Nano Lett*., **10**, 291 (2010).
28. Gramotnev D.K. *J. Appl. Phys*., **98**, 104302 (2005).
29. Vernon K.C., Gramotnev D.K., Pile D.F.P. *J. Appl. Phys*., **103**, 034304 (2008).
30. Gramotnev D.K., Pile D.F.P., Vogel M.W., Zhang X. *Phys. Rev. B*, **75**, 035431 (2007).
31. Landau L.D., Livshits E.M. *Electrodynamics of Continuous Media* (Oxford: Pergamon Press, 1984; Moscow: Nauka, 1986).
32. Novotny L., Hecht B. *Principles of Nanooptics* (Cambridge: Cambridge Univ. Press, 2006).
33. Sasaki K., Koshioka M., Misawa H., Kitamura N., Masuharaa H. *Appl. Phys. Lett*., **60**, 807 (1992).
34. Gahagan K.T., Swartzlander G.A., Jr. *Opt. Lett*., **21**, 827 (1996).
35. Johnson P.B., Christy R.W. *Phys. Rev. B*, **6**, 4370 (1972).
36. Yannopapas V., Modinos A., Stefanou N. *Opt. Quantum Electron*., **34**, 227 (2002).
37. Li K., Stockman M.I., Bergman D.J. *Phys. Rev. Lett*., **91** (22), 227402 (2003).
38. Beermann J., Novikov S.M., Sondergaard T., Rafaelsen J., Pedersen K., Bozhevolnyi S.I. *J. Opt. Soc. Am. B*, **28**, 372 (2011).
39. Lebedev V.S., Kuznetsova T.I., Vitukhnovskii A.G. *Dokl. Akad. Nauk., Ser. Fiz*., **51**, 542 (2006).
40. Dintinger J., Martin O.J.F. *Opt. Express*, **17**, 2364 (2009).
41. http://www.comsol.com/ products/multiphysics/.
42. Palik E.D. *Handbook of Optical Constants of Solids* (New York: Acad. Press, 1985).